

## Insights into Metal Framework Constructions from the Syntheses of New Scandium- and Yttrium-Rich Telluride Compounds: $Y_5Ni_2Te_2$ and $Sc_5PdTe_2$

Paul A. Maggard and John D. Corbett\*

Department of Chemistry  
Iowa State University  
Ames, Iowa 50011

Received August 3, 2000

Remarkable structural relationships are evident in the condensation of rare-earth-metal (R) chains in  $Gd_3MnI_3$  to metal sheets in  $Y_5Ni_2Te_2$  and to chains in  $Sc_5Ni_2Te_2$  as well as for the reaction of Pd with pairs of metal chains in  $Sc_2Te$  to give heterometal ruffled sheets in  $Sc_6PdTe_2$ . The different pathways appear to be governed principally by the relative strengths of R–R vs R–M heterometal interactions.

The nature of stable metal frameworks has been investigated since early works of Zintl, Pauling, and others.<sup>1</sup> Examples of low-dimensional metal–metal-bonded solids number in the hundreds, yet an ongoing problem is the interconnection of these within a coherent chemical and structural framework. The large field of related ternary compounds that contain a late transition metal interstitial affords wider views of structural principles,<sup>2–4</sup> and here we report even broader structural interrelationships among new chalcogenide systems.

The new metal-rich compounds reported here were synthesized via typical high-temperature solid-state chemical reactions<sup>5</sup> and characterized by single-crystal X-ray diffraction methods.<sup>7</sup> The section of the  $Y_5M_2Te_2$  ( $M = Fe, Co$  or  $Ni$ ) structure shown in Figure 1 for Fe contains heterometal layers that are infinite in projection and along  $b$ . The Y atoms alternate by  $a/2$  in depth and generate body-centered cubes of Y and puckered 6-rings that sandwich two types of M atoms (shaded). Both M atoms center trigonal prisms of yttrium (vertical in Figure 1) that generate zigzag chains of M atoms, spaced at 2.30 Å for Fe, through sharing of rectangular faces. The intermetallic layers are separated by tellurium atoms. Extended Hückel band calculations indicate that the overlap population (OP) for the shortest Y–Y interlayer interaction (3.78 Å) is only 25–30% the values for intralayer bonds ( $\sim 0.23$ ), an effect seen before in similar<sup>6</sup> structures. The total bonding about Fe can be described in terms of OP values of 0.29 for each Fe–Fe bond together with OP values (on a different scale) of 0.24–0.29 each for six Fe–Y contacts.<sup>9</sup>

A major point of this work is shown in Figure 2, the broad structural interrelationships between  $Gd_3MnI_3$ <sup>10</sup> (top),  $Y_5Ni_2Te_2$

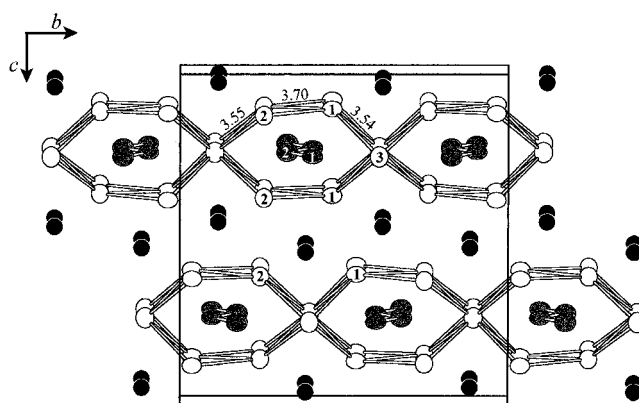


**Figure 1.** A section of the infinite heterometal sheets in  $Y_5M_2Te_2$  ( $M = Fe, Co, Ni$ ) (99.9% probability ellipsoids). Y–Y distances in Å are for the Fe analogue. Dark atoms are Te; shaded, M; open, Y.

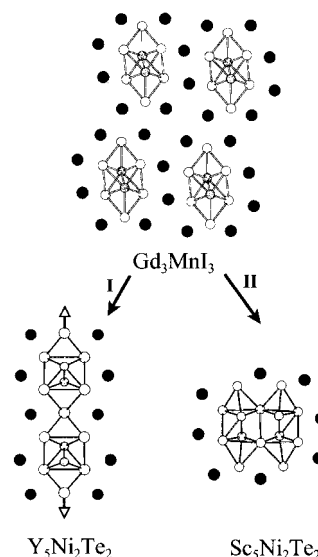


**Figure 2.** Condensation of the single 1D chains in  $Gd_3MnI_3$  into (I) sheets in  $Y_5Ni_2Te_2$  and (II) infinite double chains in  $Sc_5Ni_2Te_2$ . Unfilled atoms are Sc, Y, or Gd; shaded, Ni or Mn; black, Te or I. All are projections along the short axis of infinite chains or sheets. The process in both can be viewed as  $2R_3MI_3 \rightarrow R_5M_2Te_2 + RTe$  after substitution of one Te for each two I ( $R =$  rare-earth element).

(lower left), and  $Sc_5Ni_2Te_2$ <sup>6</sup> (lower right). The parent  $Gd_3MnI_3$  structure contains isolated metal chains identical in construction to those making up  $Y_5Ni_2Te_2$  and  $Sc_5Ni_2Te_2$ , infinite zigzag chains of late 3d metals bonded within trigonal prisms of the group 3 metal. Until now the relationship of the  $Gd_3MnI_3$  structure to anything else has been nil, but the conceptual conversions both follow the process:



$$(R = Gd, Y \text{ or } Sc; M = Mn \text{ or } Fe, Co, Ni)$$

wherein replacement of  $2I^-$  by  $Te^{2-}$  is followed by condensation and the loss of  $RTe$ . The condensation of the 1-D chains in  $Gd_3MnI_3$  takes place either through sharing of (I) trans vertices to give the  $Y_5Ni_2Te_2$  layer structure, or (II) adjacent vertices to yield the  $Sc_5Ni_2Te_2$  arrangement. The first results in polymerization of the rods into sheets, while the second halts at the dimer stage. The type I condensation results in four additional Y–Y contacts per chain repeat, while type II yields two more Sc–Sc and two Sc–Ni interactions per repeat. Qualitatively, the choice

(1) (a) Zintl, E. *Angew. Chem.* **1939**, 52, 1. (b) Pauling, L. *Phys. Rev.* **1938**, 54, 899. (c) Pearson, W. B. *The Crystal Chemistry and Physics of Metals and Alloys*; Wiley-Interscience: New York, 1972. (d) Nesper, R. *Angew. Chem., Int. Ed. Engl.* **1991**, 30, 789.

(2) Wang, C.; Hughbanks, T. *Inorg. Chem.* **1996**, 35, 6987.

(3) Kleinke, H.; Franzen, H. F. *J. Alloy Compd.* **1996**, 238, 68.

(4) Kleinke, H. *J. Alloy Compd.* **1998**, 270, 136.

(5)  $Y_5(Fe,Co,Ni)_2Te_2$  were synthesized from pressed pellets of  $Y_2Te_3$ , yttrium, and Fe, Co, or Ni. The synthetic techniques<sup>6</sup> involve the use of welded tantalum tubes as containers that were heated to 1050 °C for 84 h. Guinier powder patterns revealed 75–95% yields, with small amounts of YTe as a side product.  $Sc_6PdTe_2$  was synthesized from a similar pellet at 1050 °C for 72 h, which gave ~85% yields plus small amounts of ScTe.

(6) Maggard, P. A.; Corbett, J. D. *Inorg. Chem.* **1999**, 38, 1945.

(7) Single-crystal data were collected on Rigaku AFC6R and Bruker CCD diffractometers to  $2\theta_{max} \leq 56^\circ$ , from which *Cmcm* (No. 63) and *Pnma* (No. 62) space groups were indicated, respectively. Absorption effects were corrected by two  $\psi$ -scans and by SADABS,<sup>8</sup> respectively. Direct methods and Fourier mapping were used to locate all atomic positions, and anisotropic refinements converged at  $R(F)/R_w = 4.6/4.2\%$  and  $R1/wR2(F^2) = 2.8/7.3\%$ , respectively. The parameters and distances for each are in the Supporting Information.

(8) Blessing, R. H. *Acta Crystallogr.* **1995**, A51, 33.

(9) A more detailed structural and electronic analysis of the  $Y_5M_2Te_2$  phases and a report on a hydride derivative of the Ni phase will be forthcoming.

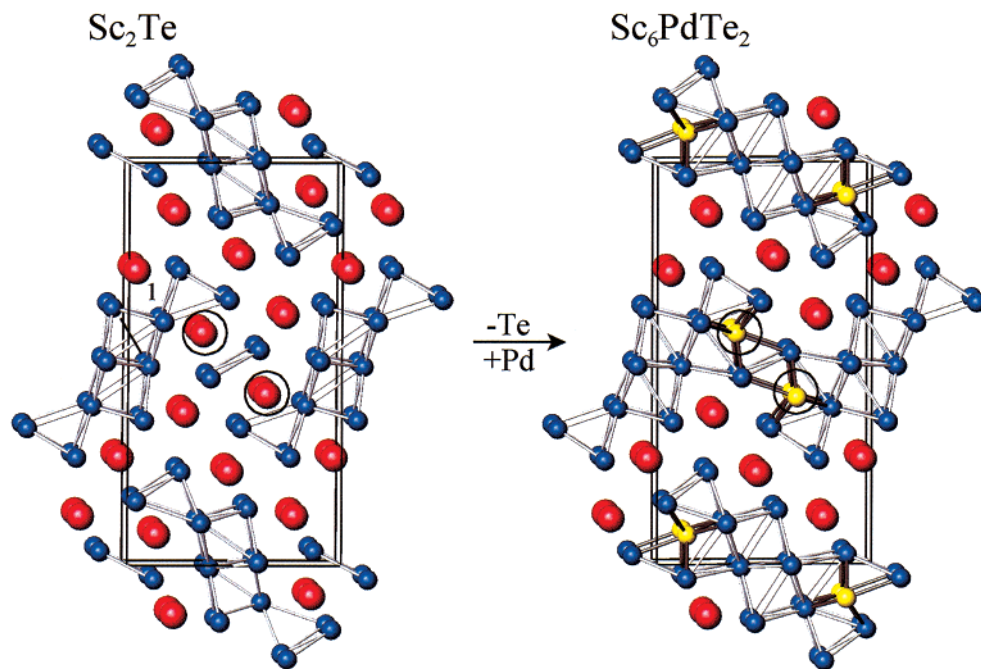


**Figure 3.** Generation of  $\text{Sc}_6\text{PdTe}_2$  (right) from  $\text{Sc}_2\text{Te}_3$  (left) by substitution of Pd for one type of Te. Sc - blue, Te - red, Pd - yellow.

appears to originate with energetic differences expected for the gain of early–early vs early–late transition metal bonding; framework metals from the early 4d and 5d periods are known to form stronger homoatomic bonds than do the corresponding 3d metals.<sup>11</sup> In other words, stronger R–R interactions favor I, while stronger R–M interactions favor II, where stronger and weaker are inferred from bond population analyses. The new (Gd,-Dy)<sub>5</sub>Ni<sub>2</sub>Te<sub>2</sub> analogues of Y<sub>5</sub>Ni<sub>2</sub>Te<sub>2</sub> are also consistent with this trend.<sup>12,13</sup> It should be obvious that theoretical treatments of the electronic changes represented in Figure 2 are a good deal more difficult than this geometric approach.

Another unexpected structural interrelationship was revealed on attempts to substitute Pd for Ni in  $\text{Sc}_5\text{Ni}_2\text{Te}_2$ , Figure 3. This led instead to  $\text{Sc}_6\text{PdTe}_2$ , the first example of heterometal-induced condensation or polymerization of metal chains, blades, etc., here in  $\text{Sc}_2\text{Te}$ <sup>14</sup> via



The reactant  $\text{Sc}_2\text{Te}$  shown in projection on the left contains both large complex and simple zigzag chains of scandium atoms (blue). The larger unit comprises quasi-infinite chains of pairs of distorted trans-edge-sharing metal octahedra, further condensed on opposite edges with trans-edge-sharing square pyramids. The new  $\text{Sc}_6\text{PdTe}_2$ , Figure 3 right, has the same space group, unit cell, and basic atom distribution except that d<sup>10</sup> palladium atoms (yellow) have replaced the circled telluride that separated the two chains, stitching the Sc “blades” and the zigzag chains into ruffled bimetallic sheets. The Sc–Pd distances to the vertices of a distorted trigonal prism of Sc (normal to the page) vary over 2.78–2.83 Å and to the Sc atoms that formally cap the rectangular faces, 2.91–3.33 Å, close to those about that point in  $\text{Sc}_2\text{Te}$ . Internal Sc–Sc distance trends remain similar to those in  $\text{Sc}_2\text{Te}$ .

(10) Ebihara, M. Martin, J. D.; Corbett, J. D. *Inorg. Chem.* **1994**, *33*, 2078.

(11) Franzen, H. F.; Köckerling, M. *Prog. Solid State Chem.* **1995**, *23*, 265.

(12) Herle, P. S.; Corbett, J. D., to be submitted for publication.

(13) Comparable interpretations of heterometal bonding effects in terms of the degree of energy matching have been advanced for interstitial-centered cluster halides of the rare-earth metals: Köckerling, M.; Martin, J. D., *Inorg. Chem.*, accepted.

(14) Maggard, P. A.; Corbett, J. D. *Angew. Chem. Int. Ed. Engl.* **1997**, *18*, 11974.

Palladium substitutes in a portion of the  $\text{Sc}_2\text{Te}$  structure where Sc–Sc bond populations are low relative to the distances, replacing Sc–Te matrix effects and polar bonding with more covalent Sc–Pd bonds as the energy matching of the interacting orbitals became better and additional valence orbitals on Pd are added. Nonetheless, an appreciable difference in Sc 3d – Pd 4d orbital energies remains, so that the bonding does not disrupt the Sc network as it does in  $\text{Sc}_6\text{NiTe}_2$  (below). A secondary effect of the stronger Sc1–Pd interactions is that the proportions of the condensed double octahedra have switched roles. The seeming chemical equivalency of Pd and Te in this chemistry has some analogues in other system as well, namely that the 3d metal and the nonmetal in  $\text{Hf}_5\text{Co}_{1+x}\text{P}_{3-x}$ <sup>3</sup> are mixed within trigonal prismatic sites of Hf and likewise in Zr sites in  $\text{Zr}_6\text{Fe}_{0.6}\text{Se}_{2.4}$ .<sup>2</sup> These effects may be more size- than orbital-dependent; all of these substrates are metallic so that the electron count changes are not so important. The general loss of R–R metal bonding with gains to M neighbors is also found in the contrasting  $\text{R}_6\text{MTe}_2$  (R = Sc, Dy; M = Mn, Fe, Co, Ni)<sup>15</sup> which crystallize in an ordered  $\text{Fe}_2\text{P}$  type with clearly stronger R–M d orbital interactions in centered trigonal prisms of R. More detailed structural and electronic analyses are forthcoming in full papers, the emphasis here being the insightful structural relationships that assist our understanding of the formation and stability of metal frameworks.

**Acknowledgment.** This work was supported by the National Science Foundation, Solid State Chemistry, via Grant DM-9809850 and was carried out in the facilities of the Ames Laboratory, U.S. Department of Energy.

**Supporting Information Available:** Tables of crystallographic and atomic parameters and nearest neighbor distances in  $\text{Y}_5\text{Fe}_2\text{Te}_2$  and  $\text{Sc}_6\text{PdTe}_2$  (PDF). This material is available free of charge via the Internet at <http://pubs.acs.org>.

JA002875J

(15) Maggard, P. A.; Corbett, J. D. *Inorg. Chem.* **2000**, *39*, 4143; Bestaoui, N.; Herle, P. S.; Corbett, J. D. *J. Solid State Chem.* **2000**, in press.